Hexaferrite Substrate Versus Impedance Matching for Tuneable Patch Antenna Miniaturisation

Oliver Norman James, Geoff Hilton, Mark Beach
Communications Systems and Networks Group, University of Bristol, United Kingdom. oliver.james@bristol.ac.uk

***Abstract*—Novel hexaferrite substrates and impedance matching networks are both means to deliver electrically small antennas (ESAs). The performance characteristics of each are often restricted to a discussion on the reflection coefficient S11, without consideration of full radiative characterisation. In this work the radiation efficiency and pattern of a hexaferrite patch ESA and impedance-matched sub-resonant Rogers RT5880 patch were compared. The efficiencies of each technique were found to be low, while the pattern of the sub-resonant patch displayed considerable divergence from the half-wavelength behaviour of the hexaferrite patch. The stability of the magnetically-tuned radiation pattern of the hexaferrite patch was then demonstrated over a tuned bandwidth of 32.1%.**

***Index Terms*—Electrically small antennas, hexagonal ferrite, reconfigurable antennas, tuning, UHF antennas.**

I. Introduction

Hexagonal ferrites (HXFs) continue to be proposed as an avenue for miniaturisation of antennas in various form factors, particularly in the frequency range associated with the upper VHF and lower UHF bands [1], [2], [3], [4], [5], [6]. Their intrinsic magneto-dielectric (MD) behaviour permits antenna miniatursation of the antenna through not only increased substrate dielectric permittivity ε_{r}, but also increased magnetic permeability μ_{r} relative to that of the vacuum [2]. While the measured input response of various proposed antennas has indicated that miniaturisation of the antenna was successfully achieved for a number of designs [3], [2], [4], [5], [6], radiative characterisation of the realised radiation performance of hexaferrite antennas with high filling factors such as patches have suggested that the loss tangents $\tan\delta_{\varepsilon}$ and $\tan\delta_{\mu}$ of hexaferrite materials do not favour use in long-range transmission applications [1], [6].

However, while high material loss tangent has a major effect on the substrate losses in the antenna hence reducing the radiation efficiency [1], a comparison to relevant alternative techniques such as impedance matching networks to achieve the same electrical size as the hexaferrite option is not known to have been considered to date. Impedance matching of electrically small antennas (ESAs) is recognised to be difficult due to the increased reactance of ESA structures resulting in narrow instantaneous bandwidth, however a degree of flexibility is also created in the impedance-matched antenna design if tuneable matching networks are subsequently used to increase the operating bandwidth of the ESA.

Impedance matching as a miniaturisation technique therefore warrants investigation as an alternative to the use of hexaferrite materials, as both techniques offer antenna miniaturisation and frequency reconfigurability, considering that hexaferrite materials are typically held to be magnetically tuneable due to their ferromagnetic phase at appropriate system temperatures (e.g. 293 K).

In this work, the respective radiation performances of hexaferrite- and matching-miniaturised patch ESAs were compared. A hexaferrite patch antenna described in [1] was compared to an equivalently-sized Rogers RT5880 substrate-based patch with and without the use of an impedance matching network reducing the operating frequency of the RT5880 antenna to an electrically small regime (ka reduction from 2.11 to 0.30). The input response, radiation pattern and radiation efficiency were measured and analysed. Subsequently, the frequency-reconfigurable behaviour of the hexaferrite antenna was determined through magnetic biasing of the material, while the radiation efficiency and pattern were recorded at the extremes of the tuning range. Development of a tuneable matching network addressing the same tuned frequency range as the hexaferrite antenna is an option deferred to future works.

II. Background review

A. Hexagonal ferrite antennas

The motivation for the production of the hexaferrite patch antenna featured in this work was previously presented in [1]. To review, theoretical lossless MD patch antennas were treated in [7], wherein the patch antenna bandwidth was noted to degrade more slowly with increasing miniaturisation if increasing μ_{r} was used to provide some of the miniaturisation, in constrast to increasing ε_{r} alone. HXFs are MD materials, which compared to spinel and Ni-Zn ferrites offer greater control over the values of μ_{r} and ε_{r} with respect to the frequency limits beyond which extremely lossy ferromagnetic resonance mechanisms dominate the material behaviour [2]. The controllable MD behaviour of HXF materials has been the basis of various antenna designs such as wire-conductor stimulated hexaferrite chips [3], conductors encased in hexaferrite [2], patches with solid-tile substrates [4], [5] and flexible substrates [6].

While all of these works reported antenna miniaturisation in terms of frequency reduction in the S_{11} value of the input response, the varying treatment of loss tangent and efficiency concerns caused differing conclusions on the applicability of the antenna to various communication problems. The initial characterisation of the radiative performance of the patch with HXF substrate [1] featured in this work led to the conclusion

that hexaferrite patches are mostly applicable to short range communications. This was consistent with the view of [6] which advanced RFID and health monitoring as potential applications, where the miniaturisation is of crucial importance for user acceptance compared to the lesser concern of radiated efficiency.

B. Sub-resonant impedance matching

The low realised radiation efficiency of the HXF substrate approach warrants a review of alternative miniaturisation techniques to be subjected to similar radiative characterisation. Impedance matching as a means to achieve electrically small antenna operation has been proposed in various works e.g. [8], [9], [10]. The difficulty of impedance matching an ESA structure is increased by the increasing reactance of the structure as electrical size is decreased, reducing the instantaneous bandwidth over which an acceptable match is found [8]. Non-Foster matching approaches permit broadening of the bandwidth [8], while tuneable matching can sweep a narrowband response over a broad range [9], potentially allowing recovery from reactive impedance mismatch caused by hand-effect detuning in compact communications terminals [11].

Nonetheless, improved impedance matching is not a guarantor for enhanced total system efficiency, given the potential for loss in the matching components and the small aperture occupied by the ESA conducting element. Opinions on the effect of improved impedance matching on system efficiency range from statements that "radiation performance is good... as long as [the ESA] is matched" [10], to observation that inefficiency of the matching network varies with antenna efficiency, which necessitates total system efficiency measurement [12]. Moreover, the radiation pattern established from matching for an arbitrary frequency can also be overlooked. The work of [8] showed that the emplacement of matching components on the ESA structure can affect the radiation pattern directly, the potential for which was overlooked in e.g. [9] despite including variable loading on the ends of a spiral, creating the potential for direct modification of the current distribution.

In this work, the ESA was a patch antenna which is generally held to be a naturally resonant $\lambda/2$ device offering broadbeam pattern coverage [13]. Impedance matching the antenna to a sub-resonant state does not preserve the $\lambda/2$ boundary condition under miniaturisation, risking resultant undesirable pattern corruption. Conversely, miniaturisation effected by use of MD substrate such as HXF maintains a patch length of $\lambda/2$ despite being an ESA structure. Thus, an objective comparison of the pattern performance of each technique is warranted.

C. Ferromagnetic tuning in hexaferrites

The HXF material featured in this work was susceptible to tuning of the permeability μ_r under application of an external magnetic bias field. To date, the frequency-reconfiguration of a comparable hexaferrite patch antenna through magnetic biasing appears only to have been addressed in the work [5], but this was not accompanied by a radiative characterisation of the efficiency or pattern across the tuned band.

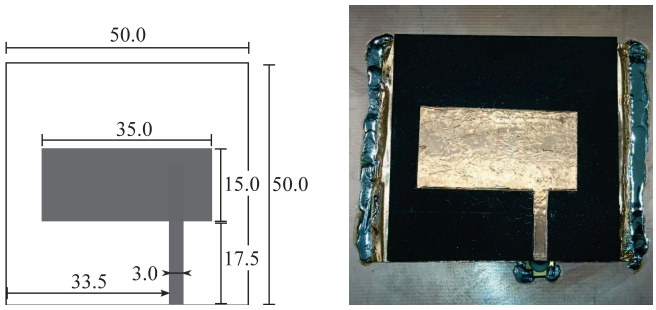

Left: patch dimensions (mm). Right: Fabricated patch.

Fig. 1. Hexaferrite patch antenna design.

As such, the overall effect of increasing ka in a tuneable HXF patch antenna is not known. For a radiation efficiency ratio $\eta_\Omega = r_\mathrm{rad}/(r_\mathrm{rad} + r_\mathrm{losses})$, the radiation resistance term r_rad should increase with increasing frequency due to the antenna's increasing Wheeler radiansphere occupancy coincident with rising ka, where $k = 2\pi/\lambda$ and a is the radius of the smallest sphere inscribing the antenna within its limits. However, characterisation of the hexaferrite material losses [1] revealed the loss tangents to be highly frequency-dependent, with generally increasing loss as a function of frequency. Thus, assumptions of increased realised antenna efficiency based on increased ka alone cannot be guaranteed to be valid, demonstrating the need for measurement of the radiation efficiency in tuneable-substrate miniaturisation solutions.

III. Sub-resonant impedance-matched antenna

A. Design

The hexaferrite patch antenna examined here was designed using dimensions and a substrate first detailed in [1]. The antenna dimensions are detailed in Figure 1. The main substrate material parameters at 450 MHz were $\varepsilon_\mathrm{r} = 15.1$, $\mu_\mathrm{r} = 11.3$, $\tan\delta_\varepsilon = 0.19$, $\tan\delta_\mu = 0.18$. A pair of equivalently sized antennas were also fabricated on RT5880 substrate ($\varepsilon_\mathrm{r} = 2.3$, $\tan\delta_\varepsilon = 0.0003$ across 1–1000 MHz) with and without an impedance matching network (Figure 2).

The target impedance for matching the RT5880 to a frequency close to 450 MHz was determined from a simulation of the naturally-resonant RT5880 structure in CST Microwave Studio. This allowed a preliminary simulation of ideal-valued matching topologies to be tested to confirm the existence of a physically-realisable matching solution. The chosen matching solution was a three-stage 'L' network topology, gradually matching the unmatched load impedance of 0.25-24.6j Ω at 450 MHz to the 50 Ω feed line. However, simulated ideal L and C components in arbitrary values cannot be used for practical matching. A re-simulation of the matching network in Keysight ADS using manufacturer-provided S-parameter models of preferred-value matching components and actual microstrip track effects indicated the fabricated antenna would be well-matched at 410 MHz (Figure 3), a frequency point within 10% of the 450 MHz goal. This was considered acceptable for an attempted proof-of-concept demonstration for

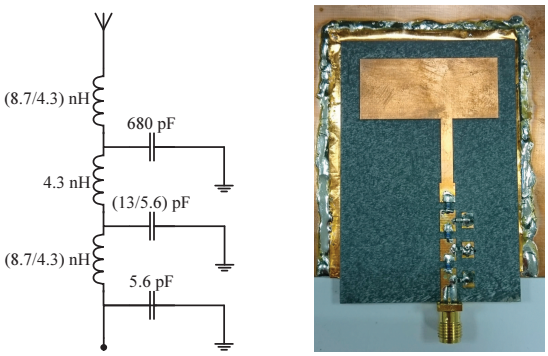

Left: matching network with (simulation/fabricated) values.

Right: fabricated matched patch.

Fig. 2. Sub-resonant RT5880 patch antenna matching network.

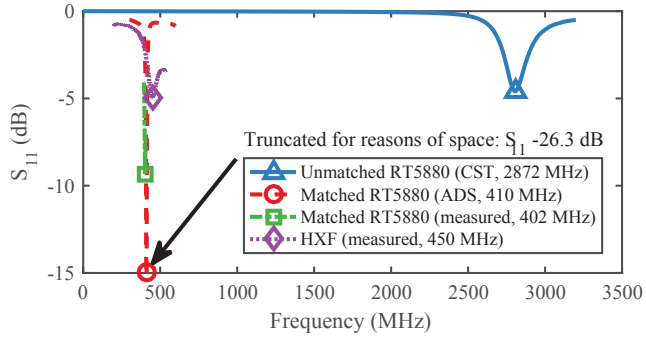

Fig. 3. Measured reflection coefficient of impedance-matched and substrate-based miniaturisation solutions.

characterisation of the sub-resonant RT5880 patch antenna in an electrically small regime. The fabricated antenna with impedance matching was found to have an impedance matching efficiency $\eta_{\mathrm{m}} = 1 - \Gamma^2 = 88\%$ (-0.5 dB) at 402 MHz (Figure 3), derived from measured S_{11} where Γ is the voltage-reflection coefficient. Thus, the operating frequency of the RT5880 patch naturally resonant at 2872 MHz was reduced to 402 MHz (a frequency reduction factor of 7.1), similar miniaturisation to the frequency reduction caused by substituting the RT5880 for hexaferrite substrate material (frequency reduction factor 6.4) described in [1].

B. Radiative characterisation

The radiative characterisation system is the same as that detailed in [1] (Figure 4). In brief, measurements of two orthogonal 3D radiation patterns were recorded for each antenna under test (AUT), as well as for a $\lambda/4$ wire monopole fabricated for each frequency. Comparison of the patterns permitted the calculation of realised radiation efficiency via a pattern integration method [14] comparing the total power received by each AUT compared to that received by a $\lambda/4$ reference monopole. From the total link strength efficiency η_{tot} measured relative to the monopole, the radiation efficiency was established from $\eta_{\Omega} = \eta_{\mathrm{tot}} \times (\eta_{\mathrm{m,\ monopole}}/\eta_{\mathrm{m,\ AUT}})$.

The respective radiation efficiencies are given in Table I. Since η_{m} is only a measure of power not reflected back

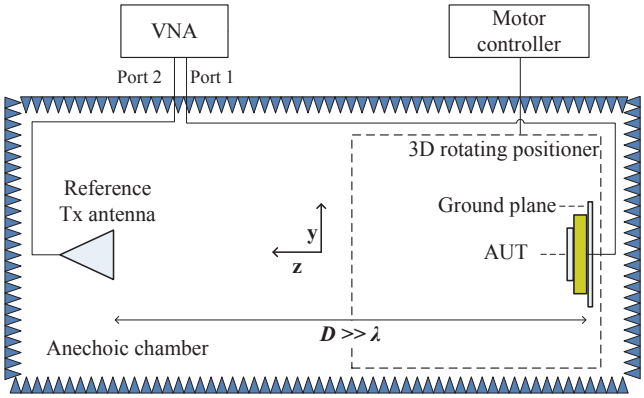

Fig. 4. Anechoic 3D radiation pattern measurement setup.

to the vector network analyser, signal loss in the matching components forms part of the radiation efficiency term, η_{Ω}. The gain is given from the efficiency and pattern information, where gain $G_{\mathrm{max}} = \eta_{\mathrm{tot}} D_{\mathrm{max}}$ with D_{max} being the maximum measured directivity.

TABLE I
REALISED EFFICIENCIES OF HXF SUBSTRATE AND SUB-RESONANT IMPEDANCE-MATCHED RT5880 PATCH ANTENNAS.

Antenna	Frequency (MHz)	η_{m} (dB)	η_{Ω} (dB)	η_{tot} (dB)	D_{max} (dBi)	G_{max} (dB)
HXF	450	-1.7	-20.1	-21.8	+6.4	-15.4
RT5880 (matched)	402	-0.5	-24.2	-24.7	+4.6	-20.1
RT5880 ($\lambda/2$)	2872	-1.9	-1.1	-3.0	+8.3	+5.3

It is seen that the radiation efficiency of the sub-resonant RT5880 patch is lower than that of the HXF patch at a similar frequency, which cannot be attributed to the loss tangent in the material since RT5880 has previously been shown to exhibit much lower loss tangent $\tan\delta_{\varepsilon}$ compared to the candidate hexaferrite [1], allowing higher efficiency when measured at its naturally-resonant $\lambda/2$ frequency in the absence of the matching network (η_{Ω} = -1.1 dB at 2872 MHz).

The low efficiency was likely caused by a combination of loss in the matching network components and poor coupling of the antenna to the far field at 402 MHz. The L and C matching components were selected for high Q, however comparison of the relevant data sheets suggests that the inductors are responsible for most of the power loss within the matching network due to lower relative Q (capacitor nominal $Q > 800$ [15], inductor nominal Q 30–50 [16]). The combined effect of reduced radiation efficiency and reduced peak directivity in the sub-resonant patch gave a +4.7 dB advantange in peak gain for the HXF patch despite the relatively high loss tangent.

The measured radiation patterns are given in Figure 5. The sub-resonant patterns were consistent with those given at 402 MHz in simulation by CST (omitted for brevity), indicating that any corruption in the pattern was an intrinsic property of the antenna rather than any spurious feed cabling effects. The

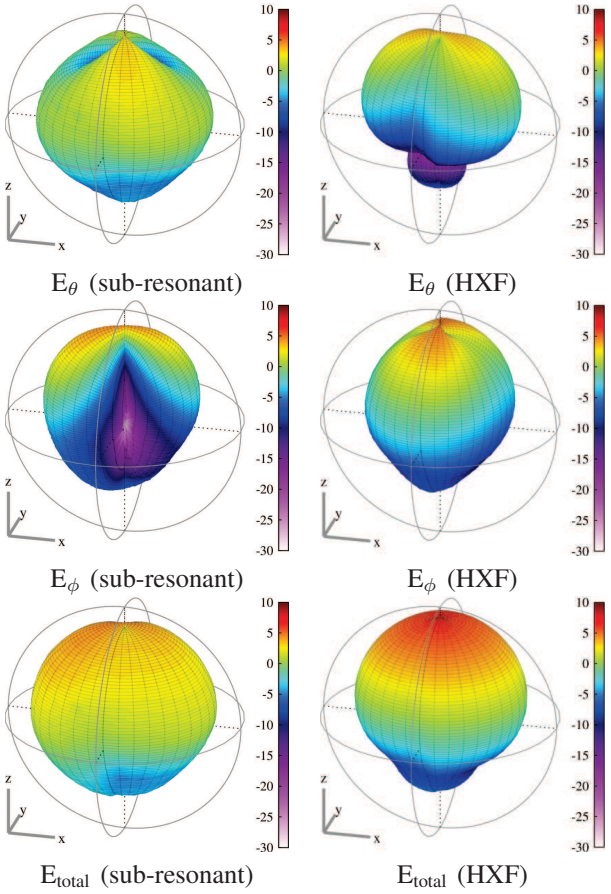

Fig. 5. Measured radiation patterns of impedance-matched and substrate-miniaturised electrically small patch antennas. The colour scale gives directivity in dBi.

patterns demonstrate that similar miniaturisation performance offered by reduced frequency in S_{11} for each miniaturisation technique is not concurrent with similar radiation pattern coverage for each technique. Rather, the HXF patch maintained the broad-beam behaviour in the forward direction ($+z$-axis) desired of patches, while the sub-resonant antenna formed two major nulls in the forward hemisphere in the E_θ polarisation. Additionally, the sub-resonant patch demonstrated significant skew in each measured polarisation considering that the antenna was mounted aligned with the axes of the xy-plane.

IV. Ferromagnetic Tuning Range

A. Magnetic bias configuration

The HXF substrate exhibits frequency reconfigurable behaviour under external magnetic biasing. A study of realised tuning range as a function of surface bias field strength was conducted by placing strong neodymium magnets on the patch conducting face (class N35 2×3 mm magnets each with nominal remanence value 1.22 T [17]). The magnets were arranged with co-polar magnetic orientation, such that the magnets repelled when pushed toward each other (Figure 6). This magnetic arrangement maximised the magnetic bias field

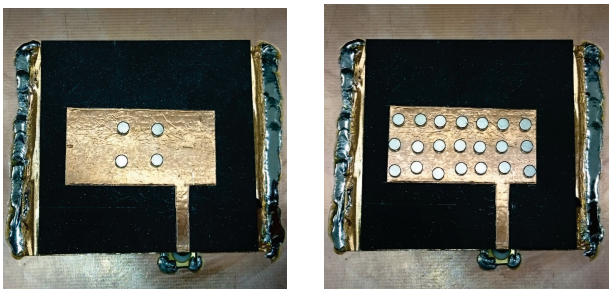

Fig. 6. Magnetic biasing of HXF patch.

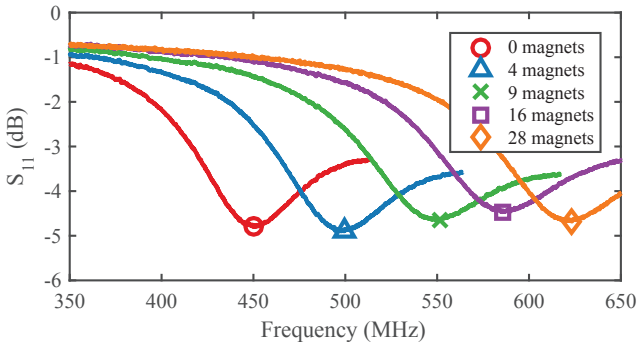

Fig. 7. Magnetically-biased tuned hexaferrite patch reflection coefficient.

TABLE II
Realised efficiencies of magnetically-tuned HXF antennas.

Antenna	Frequency (MHz)	η_m (dB)	η_Ω (dB)	η_{tot} (dB)	D_{max} (dBi)	G_{max} (dB)
HXF	450	-1.7	-20.1	-21.8	+6.4	-15.4
HXF	622	-1.8	-20.1	-21.9	+7.1	-13.0

density inside the HXF material. The number of magnets was gradually increased from zero to the maximum number which would fit on the patch face (twenty-eight), noting that the upper limit of number of magnets is dictated by the repulsion effect of adjacent co-polar magnets. The input response was found to tune over a frequency range 450–622 MHz (32.1% of centre frequency, Figure 7).

The radiation efficiency at the lower and upper limits of the tuned band were measured using the radiative characterisation procedure decribed above. The realised efficiencies given in Table II may have been expected to increase with frequency due to increased coupling of the antenna to the far-field with increasing radiansphere occupancy ka, but as observed in [1], $\tan\delta_\varepsilon$ and $\tan\delta_\mu$ also increased with frequency. This appears to have had a limiting effect on the radiation efficiency increase caused by greater r_{rad}. The radiation pattern was found to be stable across the tuning range, indicating that the same mode was stimulated throughout (power patterns given in Figure 8, polarisation patterns omitted for brevity).

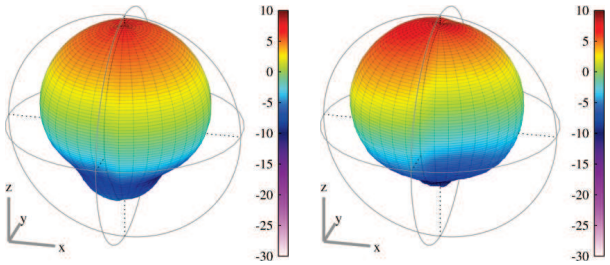

HXF (450 MHz) No magnetic bias | HXF (622 MHz) Max. magnetic bias

Fig. 8. Measured E_{tot} radiation patterns of magnetically biased HXF patches. The colour scale gives directivity in dBi.

V. Conclusions

The efficiency of an ESA patch antenna fabricated on a hexaferrite substrate has previously been shown to be adversely affected by the relatively high loss tangents compared to RT5880 substrate material [1]. Prior to the work performed here, it had not also been established whether an alternative miniaturisation technique such as impedance matching for sub-resonant antenna operation would have yielded a more efficient result. Comparison of radiated performances of the $\lambda/2$ HXF patch an impedance-matched sub-resonant RT5880 patch displayed similar values of realised total efficiency for each, despite the improved impedance matching offered for the sub-resonant patch. The HXF patch maintained preferable broad-beam pattern coverage performance compared to the RT5880 sub-resonant counterpart, with the former found to offer pattern stability over a magnetically tuned range of 32.1% bandwidth. However, radiation efficiency of the HXF patch did not increase with ka, probably due to the increasing loss tangent in the HXF material with frequency.

Based on these radiation measurements, the HXF patch is generally expected to provide superior radiation pattern coverage compared to tuned-impedance options. However, the matching topology used here is only one of many possible solutions to ESA matching, leaving room for more efficient implementations to be found. Nonetheless, the authors must stress that this measurement campaign serves as a practical demonstration of two potential flaws with antenna miniaturisation through impedance matching: first, improved S_{11} is not a guarantor of "reasonable" system efficiency, consistent with the theme of [12] requiring total system efficiency assessment. Second, improved S_{11} across a tuning range makes no guarantee of pattern stability. In this regard, the authors note the contribution of [8] highlighting the effect of matching component location on pattern. The authors recommend that designers renew their efforts to conduct radiative assessments of impedance-matched solutions for ESA design, noting particularly that the improvement in ESA S_{11} demonstrated in this work was not sufficient to predict the very low realised overall efficiency.

Acknowledgment

The authors wish to thank the UK Engineering and Physical Sciences Research Council (EPSRC) Centre for Doctoral Training (CDT) in Communications (EP/I028153/1) for financial support, and Keysight Technologies for the loan of the E4991B Impedance Analyzer used in this work.

References

[1] O. James, G. Hilton, and M. Beach, "Radiation efficiency analysis of balanced-impedance hexaferrite substrate for antenna miniaturisation," in *The Loughborough Antennas & Propagation Conference 2017 (LAPC)*, November 2017, pp. 1–5.

[2] S. Fujii, K. Wakamatsu, H. Satoh *et al.*, "Wide bandwidth CuO-modified $Ba_2Co_2Fe_{12}O_{22}$ ferrite antenna," *IEEE Antennas and Wireless Propagation Letters*, vol. 15, pp. 1171–1174, 2016.

[3] S. Bae, Y. K. Hong, J. J. Lee *et al.*, "Miniaturized broadband ferrite T-DMB antenna for mobile-phone applications," *IEEE Transactions on Magnetics*, vol. 46, no. 6, pp. 2361–2364, June 2010.

[4] Q. Zhang, Z. Chen, Y. Gao *et al.*, "Miniaturized antenna array with Co2Z hexaferrite substrate for massive MIMO," in *2014 IEEE Antennas and Propagation Society International Symposium (APSURSI)*, July 2014, pp. 1803–1804.

[5] Z. Chen, J. Yu, X. Chen *et al.*, "UHF tunable compact antennas on Co2Z hexaferrite substrate with 2.5/1 tunable frequency range," in *2015 IEEE International Symposium on Antennas and Propagation USNC/URSI National Radio Science Meeting*, July 2015, pp. 2287–2288.

[6] L. J. Martin, S. Ooi, and D. Staiculescu, "Effect of permittivity and permeability of a flexible magnetic composite material on the performance and miniaturization capability of planar antennas for RFID and wearable wireless applications," *IEEE Transactions on Components and Packaging Technologies*, vol. 32, no. 4, pp. 849–858, Dec 2009.

[7] R. Hansen and M. Burke, "Antennas with magneto-dielectrics," *Microwave and Optical Technology Letters*, vol. 26, no. 2, pp. 75–78, Jul 2000.

[8] N. Ivanov, V. Turgaliev, and D. Kholodnyak, "Performance improvement of an electrically-small loop antenna matched with non-foster negative inductance," in *2017 IEEE MTT-S International Microwave Symposium (IMS)*, June 2017, pp. 348–351.

[9] J. Zhong, A. Kiourti, and J. L. Volakis, "Increasing the efficiency of electrically small antennas across a large bandwidth using matching networks," in *2014 IEEE Antennas and Propagation Society International Symposium (APSURSI)*, July 2014, pp. 633–634.

[10] M. N. Abdallah, W. Dyab, T. K. Sarkar, and M. Salazar-Palma, "Electrically small antennas under matched conditions," in *2015 IEEE International Symposium on Antennas and Propagation USNC/URSI National Radio Science Meeting*, July 2015, pp. 1246–1247.

[11] O. J. Norman, G. Hilton, and M. Beach, "Measurement of efficiency degradation due to external detuning of a tunable patch antenna," in *2016 IEEE International Symposium on Antennas and Propagation (APSURSI)*, June 2016, pp. 2145–2146.

[12] G. Smith, "Efficiency of electrically small antennas combined with matching networks," *IEEE Transactions on Antennas and Propagation*, vol. 25, no. 3, pp. 369–373, May 1977.

[13] J. D. Kraus and R. J. Marhefka, *Antennas for all Applications*, 3rd ed. McGraw-Hill, 2002.

[14] D. L. Paul, H. Giddens, M. G. Paterson *et al.*, "Impact of body and clothing on a wearable textile dual band antenna at digital television and wireless communications bands," *IEEE Transactions on Antennas and Propagation*, vol. 61, no. 4, pp. 2188–2194, April 2013.

[15] Johanson Technology, "R14S Series 0603 Capacitor," *Datasheet*, 2017. [Online]. Available: http://www.johansontechnology.com/R14S

[16] Coilcraft Inc., "0603CS Chip Inductor," *Datasheet 195-1*, 2016.

[17] Eclipse Magnetics, "N800 Magnets," *Datasheet*, 2017. [Online]. Available: http://www.farnell.com/datasheets/612878.pdf